remote sensing

MDPI

Communication

Landslides Detection and Mapping with an Advanced Multi-Temporal Satellite Optical Technique

Valeria Satriano [1], Emanuele Ciancia [2], Carolina Filizzola [2], Nicola Genzano [1], Teodosio Lacava [2,*] and Valerio Tramutoli [1]

[1] School of Engineering, University of Basilicata, 85100 Potenza, Italy
[2] Institute of Methodologies for Environmental Analysis, National Research Council, 85050 Tito Scalo, PZ, Italy
* Correspondence: teodosio.lacava@imaa.cnr.it

Abstract: Landslides are catastrophic natural phenomena occurring as a consequence of climatic, tectonic, and human activities, sometimes combined among them. Mostly due to climate change effects, the frequency of occurrence of these events has quickly grown in recent years, with a consequent increase in related damage, both in terms of loss of human life and effects on the involved infrastructures. Therefore, implementing properly actions to mitigate consequences from slope instability is fundamental to reduce their impact on society. Satellite systems, thanks to the advantages offered by their global view and sampling repetition capability, have proven to be valid tools to be used for these activities in addition to traditional techniques based on in situ measurements. In this work, we propose an advanced multitemporal technique aimed at identifying and mapping landslides using satellite-derived land cover information. Data acquired by the Multispectral Instrument (MSI) sensor aboard the Copernicus Sentinel-2 platforms were used to investigate a landslide affecting Pomarico city (southern Italy) in January 2019. Results achieved indicate the capability of the proposed methodology in identifying, with a good trade-off between reliability and sensitivity, the area affected by the landslide not just immediately after the event, but also a few months later. The technique was implemented within the Google Earth Engine Platform, so that it is completely automatic and could be applied everywhere. Therefore, its potential for supporting mitigation activities of landslide risks is evident.

Keywords: landslides; satellite data; optical data; change detection; land cover

Citation: Satriano, V.; Ciancia, E.; Filizzola, C.; Genzano, N.; Lacava, T.; Tramutoli, V. Landslides Detection and Mapping with an Advanced Multi-Temporal Satellite Optical Technique. *Remote Sens.* **2023**, *15*, 683. https://doi.org/10.3390/rs15030683

Academic Editor: Nicola Casagli

Received: 2 December 2022
Revised: 9 December 2022
Accepted: 19 January 2023
Published: 23 January 2023

1. Introduction

Landslides are natural events responsible for huge social and economic damage worldwide [1–6], whose frequency of occurrence has greatly increased in recent years, mainly due to the effects of climate changes [7]. Italy, due to its geological, geomorphological, and hydrographic conformation, is naturally predisposed to hydrogeological instability presently widespread throughout the whole territory [3,8–10]. Among the Italian regions, Basilicata is one of the most vulnerable to landslides for its geomorphological and lithological features [11]. Many events have affected the regional territory so far contributing over the years to a depopulation of the affected areas due to the damage to civil and road infrastructures, resulting in large economic losses [11]. Different research projects tried to face the problem, studying advanced solutions to mitigate hydrogeological instability in Basilicata. Among them, a recent example is the MITIGO (Mitigazione dei rischi naturali per la sicurezza e la mobilità nelle aree montane del Mezzogiorno—Mitigation of natural risks for safety and mobility in the mountain areas of the South) project [12]. The integration of in situ and satellite data has been fostered, in this project, to provide support to the public authorities in hydrogeological and seismic risk management.

In this framework, satellite systems can be useful tools to implement mitigation and monitoring activities of landslides to support/complement traditional techniques based on in situ measurements [1,13–15]. That is possible thanks to their enhanced observation capabilities (e.g., synoptic view, spatial resolution up to a few meters, high sampling frequency, etc.), which have been further improved with the launch of the latest advanced sensors.

Over the years, both active and passive satellite sensors have been used to investigate landslide evolution by exploiting data acquired in the optical and microwave bands [13–15]. Focusing on the optical band, considering that a transition from vegetated to bare soil is usually expected after a landslide, the land cover variation change is usually the signal to be investigated by satellite to assess the phenomenon occurrence [16–19]. Land cover information is usually identified by using multispectral land cover indices (e.g., Normalized Difference Vegetation Index—NDVI, Normalized Difference Water Index—NDWI), computed by combining data in different bands within the spectral range from the Visible (VIS) to the Short Wave InfraRed (SWIR) [16–21]. The above-cited indices, exploiting the different spectral behavior of the vegetation with the other elements present in the scene, especially the high reflectance peak shown in the Near Infrared (NIR) region, can highlight the different land covers over a specific satellite image in addition to vegetation [16,17,20,21]. Furthermore, to better highlight the land cover variation, a combination of two images acquired at different times (usually pre- and post-event) are used to provide useful information about a landslide occurrence and its main features. The NDVI change calculated by differencing pre- and post-event images is indeed a powerful indicator of vegetation change due to landslides, with negative values of this difference indicating a decrease in vegetation, whereas positive ones indicate an increase [18,19]. This approach is typically applied after the event for an *a posteriori* detection [22,23], also using more than one image to monitor the landslide movement [15,23]. The main limitation of almost all the optical techniques developed so far for landslide investigation based on the above-mentioned approach (e.g., [17,22–27]) is the use and application of fixed thresholds for discriminating different land cover types, both to a single image as well as on imagery combination within multitemporal analyses. This approach makes these techniques poorly automatic and difficult to export to areas with different characteristics from those where they have been calibrated/validated. Moreover, like all the methods based on fixed thresholds, they can suffer from sensitivity accuracy/false alarm proliferation. The application of low threshold values on the considered signal (e.g., NDVI) can indeed generate a proliferation of false positives, and, on the contrary, using high values can produce a reduction in the detection accuracy.

To face all these issues, in this paper, we introduced a new approach based on a multitemporal analysis of the data acquired by Multispectral Instrument (MSI), the optical sensor onboard the Copernicus Sentinel-2 platforms [28]. With a spatial resolution up to 10 m, a temporal one of 5 days by combining two platforms (i.e., Sentinel-2A and -2B, respectively) and 12 bands in the VIS-SWIR spectral interval, this instrument has the capability of detecting short-time (namely not lower than 5 days) land cover changes. The proposed technique is based on a general multitemporal differential approach, the Robust Satellite Techniques (RST, [29]), able to identify at a pixel level and different confidence levels, statistically significant variations of the investigated signal, thus resulting indifferent to the above-mentioned limitations of fixed threshold approaches. The method, here implemented for the first time to investigate this kind of phenomenon, has been tested to analyze the landslide that occurred in Pomarico city (Matera Province, Basilicata Region, Italy) on 25–29 January 2019 [30–32], in the framework of the MITIGO project.

2. Materials and Methods

2.1. The Study Case

During the 2018 autumn/winter, the area of Pomarico city, located within the Matera (MT) municipality territory (Basilicata Region, southern Italy, Figure 1), was affected by very recurrent rain events [30–33]. On the night between 24th and 25th January 2019, an intense rainfall affected the already heavily compromised ground, triggering a large rotational slide (about 760 m in length, 80–100 m in width [30]) which further expanded into a channelized earth-flow along the south-west side of Pomarico ridge in the following days until causing on 29th January the collapse of some residential buildings and the main access road to the city [31] (Figure 1). The damages forced several inhabitants to evacuate the area and are still persistent on the territory. This was not the first time that the area involved by the 2019 landslide has been affected by such a phenomenon, indicating the great fragility of the territory, mainly because of the presence of a superficial sand layer [30]. On this layer, in the landslide area, native uncultivated grass was present before the event.

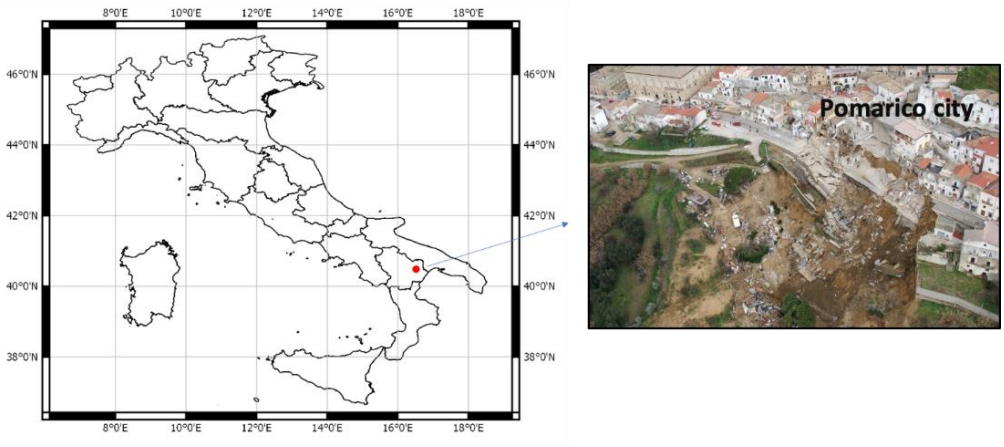

Figure 1. Pomarico city (MT) landslide location.

2.2. Data and Processing

2.2.1. Data

Sentinel-2 data, and in particular the collection MSI-Level 1C, were used in this work. The collection represents the reflectance at the Top of the Atmosphere (TOA) and is available within the Google Earth Engine (GEE) Platform [34]. A GEE *ad hoc* code was developed to perform the following preliminarily operations:

- spatial subset on the area of interest;
- temporal subset on the collection images to select the useful one/ones;
- spectral subset for the bands useful for NDVI calculation (VIS: band 4, 0.6 μm; NIR: band 8, 0.8 μm);
- NDVI estimation;
- cloud detection using the bitmask band QA60, associated with each Sentinel-2 image within the considered collection, providing cloud mask information. Only clear sky pixels (i.e., with QA60 = 0) were considered in the following analyses;
- computation of the change detection index here proposed and presented in the following section.

The exploitation of MSI 4 (VIS) and 8 (NIR) bands allows us to achieve information at 10 m spatial resolution and, hence, with an accuracy good enough to analyze phenomena such as the one investigated in this work.

2.2.2. RST-cover

The technique proposed in this paper, christened RST-cover, is based on the more general Robust Satellite Technique (RST, [35]). This approach is a general multitemporal satellite data analysis method, already used with excellent results to investigate different natural hazards [36–42]. The RST philosophy needs the preliminary characterization of the signal observed (in single bands or band combinations) in terms of expected value (temporal mean) and natural variability (standard deviation) by investigating long-term satellite data series acquired in homogenous conditions. These conditions refer to the analysis of the signal measured for the same location (i.e., pixel) in the same temporal window (i.e., hour of day, month/season of the year, etc.) under clear-sky conditions to reduce noise contributions to the identification of the expected values.

Moving to RST-cover, its main objective is to identify possible land cover changes and, for this purpose, the signal under investigation is the NDVI index. The technique has been here applied to the Pomarico landslide event, considering a historical dataset of 82 Sentinel-2 L1C data available in the period December–February from 2016 to 2018. We combined these three months considering that land cover changes at that temporal scale are almost limited. Such a sub-seasonal temporal aggregation allowed us to produce a historical dataset of MSI data large enough to guarantee a robust identification of the unperturbed conditions [43], also considering cloud coverage occurrence probability. About 25 images (i.e., 30% of the selected series) as average on the whole scene were indeed not considered because they resulted cloudy affected according to QA60 band information. In its final step, RST-cover foresees the implementation of a change detection index (ALICE—Absolutely Local Index of Change of Environment [35]), as in the following:

$$\otimes_{\mathrm{NDVI}}(x,y,t) = \frac{\mathrm{NDVI}(x,y,t) - \mu_{\mathrm{NDVI}}(x,y)}{\sigma_{\mathrm{NDVI}}(x,y)} \quad (1)$$

where NDVI is the value achieved by calculating such an index for each pixel of the investigated scene at (x,y) location and time (t); μ_{NDVI} and σ_{NDVI} are, respectively, the NDVI temporal mean and standard deviation computed on the considered dataset (i.e., December–February from 2016 to 2018) for the same pixel. As already said, the whole RST-cover process was implemented in GEE Platform. Considering the ALICE index is a Gaussian standardized variable (with the temporal mean ~0 and the standard deviation ~1), then increasing ALICE absolute values can be associated with statistically anomalous events [44]. $\otimes_{\mathrm{NDVI}}(x,y,t)$ values lower than −2, −3, and −5, indeed, indicate a decreasing occurrence probability equal to 2.27%, 0.15%, and 2.8×10^{-5}%, respectively. Lower and lower $\otimes_{\mathrm{NDVI}}(x,y,t)$ values are associated with even lower occurrence probabilities. In our case (signal distribution is quasi-Gaussian) ALICE values and probability of occurrence of NDVI anomalies in the hypothesis of a Gaussian distribution, are used just as an indication of their significance (i.e., how rare they are in the considered time series).

RST-cover can be applied to any phenomena involving land cover changes (e.g., landslides, floods, fires, vegetation diseases, etc.) by choosing, if necessary, an index different from the NDVI (e.g., the NDWI, the Soil-Adjusted Vegetation Index-SAVI, the Bare Soil Index–BSI, etc.) as well as different temporal scale data aggregation solutions (e.g., monthly rather than quarterly) or data processing approaches (e.g., the NDVI Maximum Value Composite used in [38]).

3. Results

The first cloud-free image of the landslide is 9th February 2019 at 09.40 GMT, acquired by Sentinel-2B (Figure 2). The affected area is within the red ellipse, represented mainly by the northern bright pixels along a NE-SW strip. This area should highlight the presence of bare soils, even if spectral features very similar to this one (i.e., clusters of bright pixels) are present all over the scene, making the landslide presence almost indistinguishable.

Its presence starts to become more evident for comparison with the Sentinel-2A image collected the same day (9th February) of the year before (2018) at the same local time (Figure 3). This image, collected under conditions very similar to those related to the image shown in Figure 2, has been selected as the pre-event image. In this scene, the bright pixel strip before indicated is not present, suggesting a clear land-cover change between the two images.

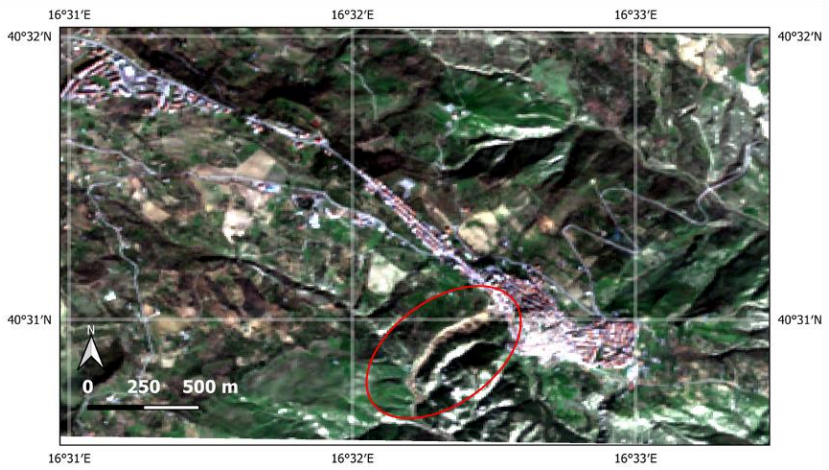

Figure 2. Sentinel-2B RGB (R = 0.665 μm (band 4), G = 0.560 μm (band 3), B = 0.490 μm (band 2)) image of 9th February 2019 at 09.40 GMT. The area affected by the landslide is in the red ellipse.

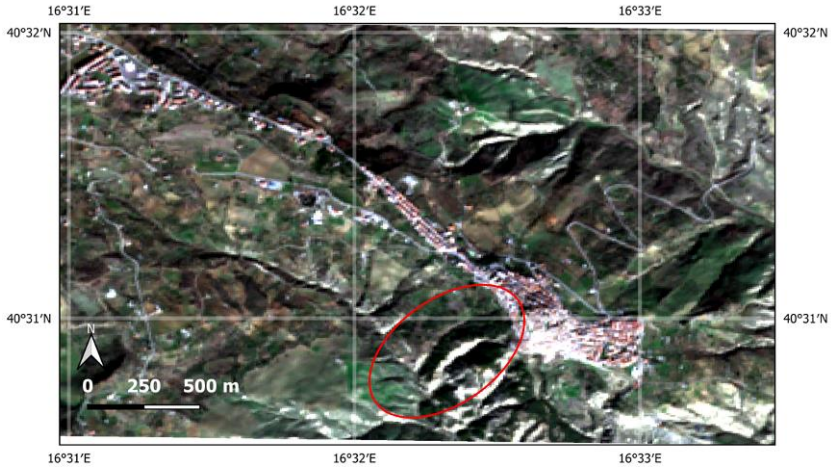

Figure 3. As Figure 2 for the Sentinel-2A image of 9th February 2018 at 09.40 GMT.

To highlight the landslide footprint, the NDVI map difference between the two above-shown images has been computed and plotted in Figure 4, while the NDVI single maps are not reported for the sake of brevity. In Figure 4, brown tones indicate a decrease in NDVI values at different levels, while green ones are related to NDVI increases. It is worth noting that in this palette, the highest extreme values are indicative of a sharp land cover change between vegetated and not soils.

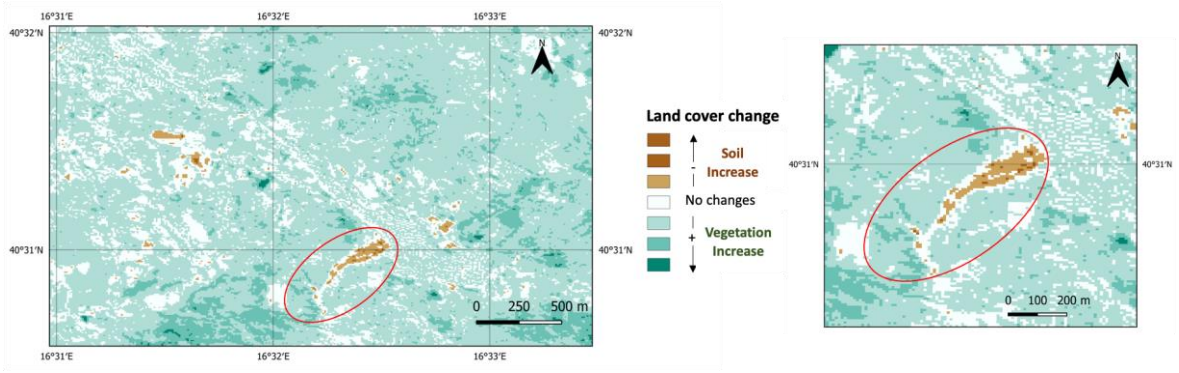

Figure 4. Map of NDVI difference between February 2019 and February 2018. The area affected by the landslide is in the red ellipse.

Focusing on the landslide area, a clear land cover variation was detected by such a simple two-image multitemporal approach. Indeed, as expected, in brown (negative values) it is possible to recognize the soil flow with a decrease in the NDVI index due to the presence of bare soil where previously there was vegetation. The main limitation of this approach is that several features, which are very similar to those highlighted in the ellipse, are present in the whole scene, which is only a small spatial subset of a large tile. In the absence of information confirming the occurrence of other phenomena like the Pomarico landslide at a larger scale (i.e., the investigated scene), these features have to be classified as false alarms in the context where we are discussing their presence. This is a big issue, limiting the ingestion of such an approach within an automatic landslide identification system.

Results achieved by implementing the index in Equation (1) for the post-image event (Figure 2) are shown in Figure 5. The $\otimes_{NDVI}(x,y,t)$ index was computed for the analyzed image, expecting negative values in correspondence with a soil increase (e.g., landslide area), and positive ones in the presence of a vegetation increase with respect to the unperturbed conditions.

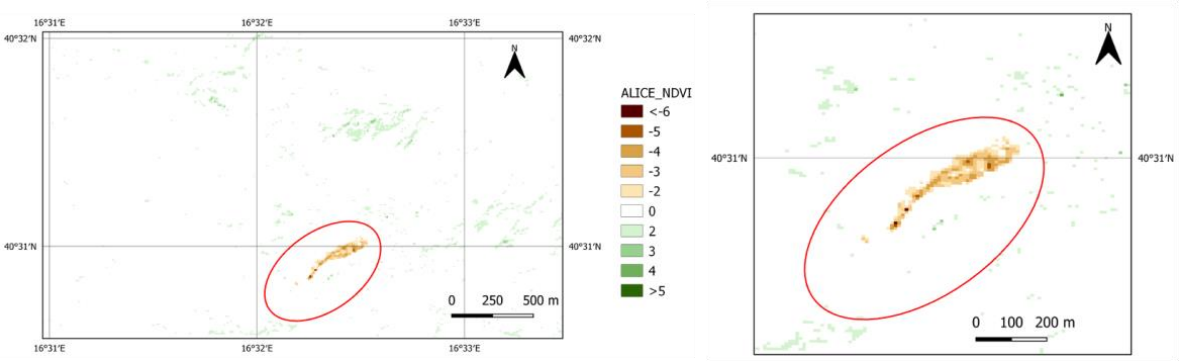

Figure 5. $\otimes_{NDVI}(x,y,t)$ computed for the Sentinel-2 L1C image of 9th February 2019 at 09.40 GMT. The area affected by the landslide is in the red ellipse.

The relevance of the obtained results is evident. The landslide area is characterized by the presence of several pixels showing statistically significant negative values of the proposed index, which means a clear deviation from the expected values (in terms of NDVI) as identified by the historical analysis. The analysis of the whole scene reveals that only a very low number of spurious pixels have been detected above the −2 $\otimes_{NDVI}(x,y,t)$ value. Such a behavior could be related to natural land-cover changes and further highlights the high intensity of the natural phenomenon that occurred in Pomarico.

The accuracy of the results just shown was assessed through the comparison with an in situ study conducted in the same area and for the same event by [31]. The vector

indicating landslide borders built during this study by a multidisciplinary approach was overlapped with the map shown in Figure 5, obtaining the output depicted in Figure 6.

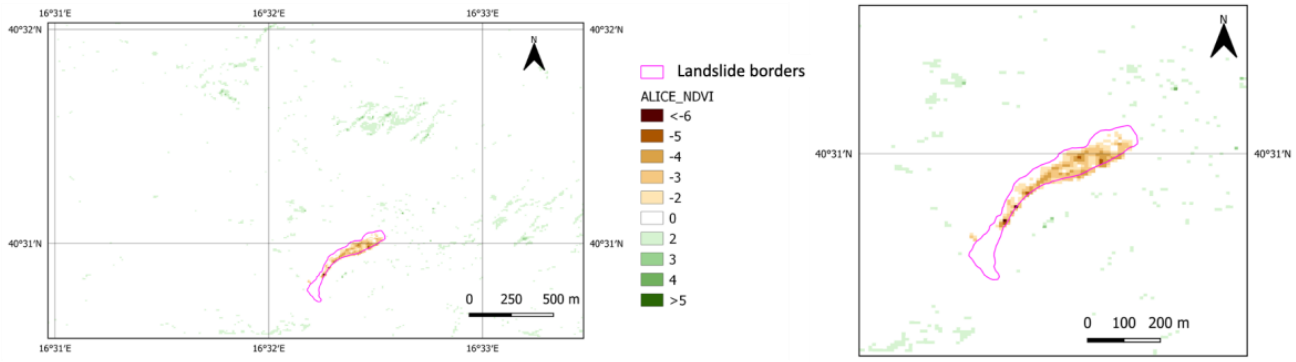

Figure 6. Landslide borders vector obtained by in-field surveys [31] overlapped with the $\otimes_{NDVI}(x,y,t)$ map image.

All the pixels detected as anomalous by the index fall within the area identified as affected by the landslide, confirming the RST-cover reliability. In any case, a discrepancy between the size of the two detected areas is evident and can be justified by different reasons. For example, the absence of RST-based identification at the landslide foot may be due to the presence of bare soil in such an area already before the event, as confirmed by looking at the pre- and post-event images (Figures 2 and 3). Moreover, the output of the in-field surveys [31] was produced later than the image used as a post-event within the proposed approach (i.e., Figure 2). Hence, a difference is expected, also taking into account that the accuracy of ground measurement is obviously higher than the one achievable by satellite. However, in any case, the results are encouraging. They may open, after the confirmation of these first results by further works focused on investigating phenomena of a different nature as well as size, to the implementation of RST-cover in a large-scale monitoring system, especially for those areas not well-instrumented or remotely located, to provide a rapid warning.

To further assess the reliability of the proposed technique, we also carried out a confutation analysis implementing RST-cover on the Pomarico landslide area for an unperturbed image, i.e., 9th February 2018 (Figure 3), namely in the absence of some known perturbation to the land-cover due to natural phenomena. The output is reported in Figure 7, where the same shapefile already shown in Figure 6 was plotted to help in focusing on the landslide area.

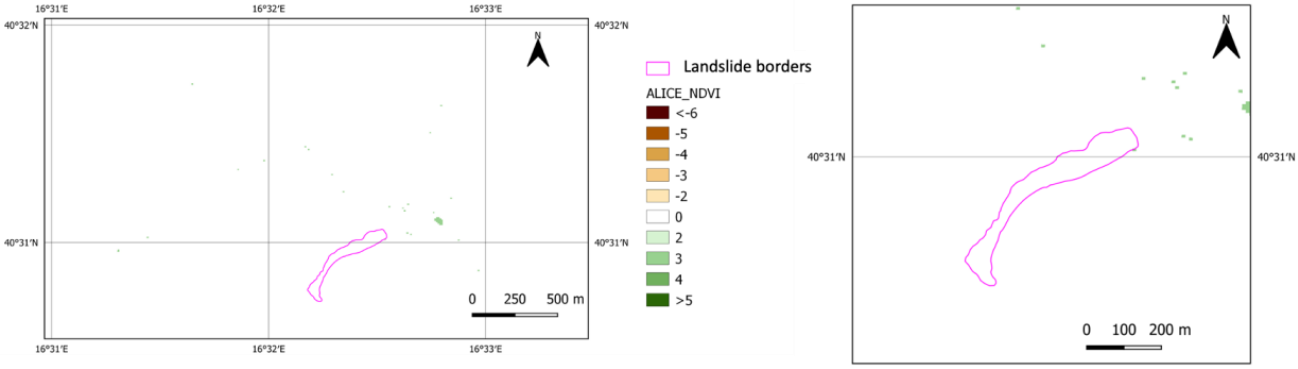

Figure 7. $\otimes_{NDVI}(x,y,t)$ computed for the Sentinel-2 L1C image of 9th February 2018 at 09.40 GMT.

No changes (positive and/or negative) have been detected in the analyzed area as well as on the whole scene, confirming the robustness of the new technique applied. The proposed methodology being fully automatic and exportable everywhere (just requiring

a sufficiently long satellite image time-series) as well as on whatever satellite sensor, its potential seems to be impressive, even if with a series of precautions about its implementation, which will be discussed in the next section.

4. Discussion and Conclusions

Landslides detection by optical satellites is still an open challenge. The existing studies apply fixed threshold change detection approaches on the NDVI land cover index [17,22–27] to recognize variation on the ground directly related to the landslide movement. As shown in Section 3, this kind of technique can identify an event but is affected by a series of false identifications when applied on a large scale, conditioning their effectiveness, as well as their capability to be automatically implemented (i.e., to detect events not otherwise already known). On the other hand, a methodology such as the one here presented has demonstrated to be able to detect a landslide without any other false identifications (Figure 5), being, for its construction, easily exportable wherever and compatible with the implementation within an unsupervised automatic detection system.

To better evaluate the potential of the technique here proposed, an analysis of the area of interest during the whole 2019 was also carried out. The aim was to assess if the proposed index can be able to detect landslide-affected pixels also during the months after the event, allowing us to follow its evolution in the spatiotemporal domain. To this aim, following the approach just used, firstly the year was split on a three-month temporal scale (i.e., March–May, June–August, September–November, plus the December–February period already analyzed), building the corresponding datasets of MSI images useful for the statistical characterization of the expected signal. Then, at least one image per month in 2019 was analyzed with the index proposed in Equation (1) to check for the presence of Pomarico landslide evidence. Information about the selected images and historical datasets is provided in Table 1. No clear sky images of the studied area were available for May 2019.

Table 1. Sentinel 2-L1C selected images and relative historical datasets.

Sentinel 2 L1C Selected Images	Historical Dataset Built
- 16 March 2019 09.40 - 20 April 2019 09.40	March–May, from 2016 to 2018 (86 images)
- 19 June 2019 09.40 - 24 July 2019 09.40 - 18 August 2019 09.40	June–August, from 2016 to 2018 (106 images)
- 22 September 2019 09.40 - 22 October 2019 09.40 - 11 November 2019 09.40	September–November,from 2016 to 2018 (107 images)

The output of this analysis is shown in Figure 8, where we focused on the landslide area highlighting only the negative values of the index.

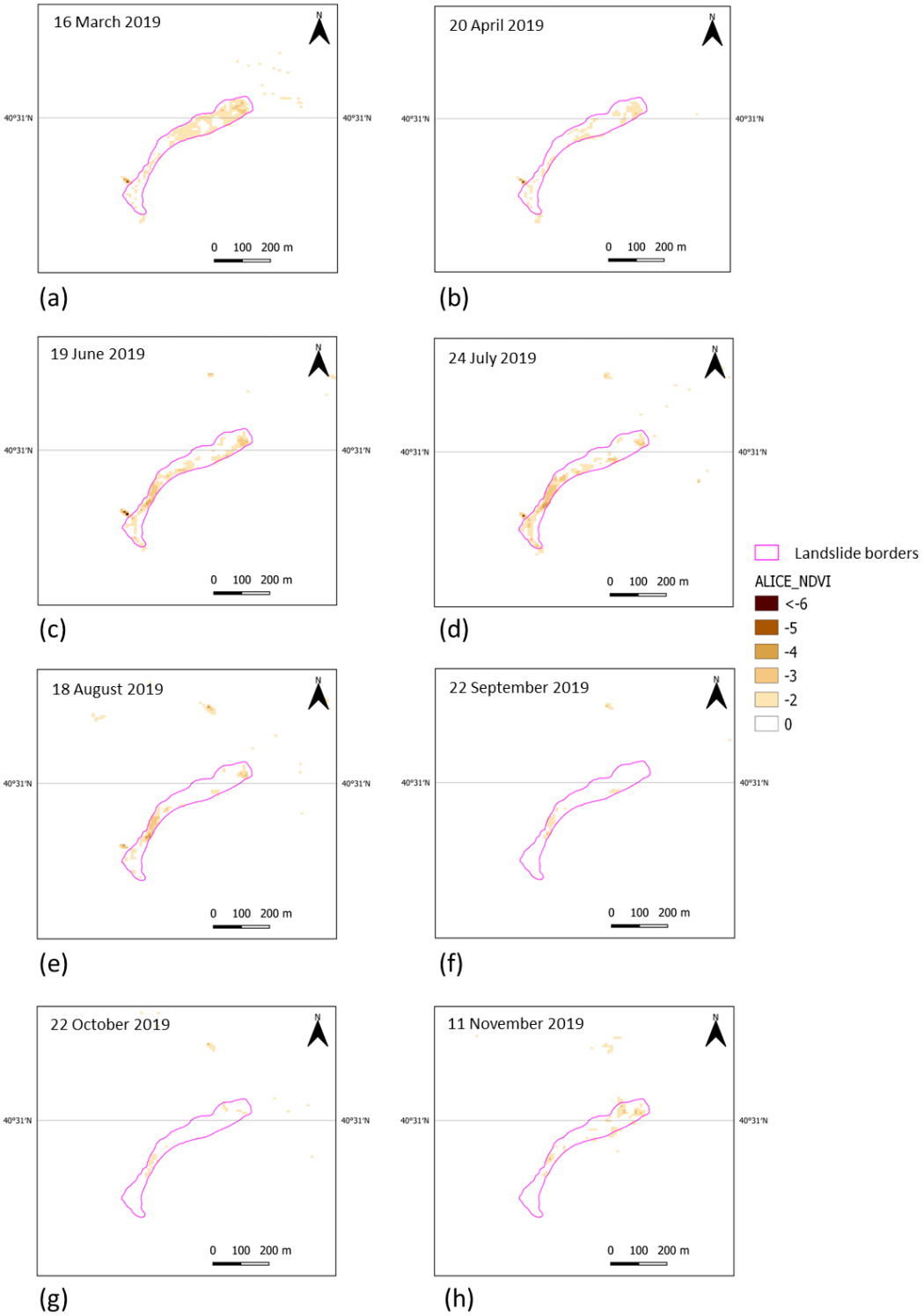

Figure 8. $\otimes_{NDVI}(x,y,t)$ computed for the following Sentinel−2 L1C images: (**a**) 16 March 2019; (**b**) 20 April 2019; (**c**) 19 June 2019; (**d**) 24 July 2019; (**e**) 18 August 2019; (**f**) 22 September 2019; (**g**) 22 October 2019; (**h**) 11 November 2019.

Effects of the perturbation due to the presence of the landslide are quite evident in all the analyzed images. The results thus obtained allowed us to follow its evolution after the event. A movement of the anomalous areas from the top to the foot of the landslide is evident, suggesting that, together with a regrowth of vegetation in the northern part, during summer, the lower section of the landslide shows conditions extremely different from

the normal ones. The strange anomalous area in the southwestern section of the landslide foot, just outside its boundary, is related to a small lake produced by the accumulation material [31], which was already present in the February 2019 image (Figure 6). Water has lower NDVI values than vegetation. Hence, its detection by means of the proposed approach is plausible. In addition, a clear trend to return to normal conditions can be observed. Over the months, there is indeed a progressive reduction of the pixels identified as anomalous, confirming that the significant variation in land cover caused by the landslide slowly gives way to a re-establishment of normal coverage ($-2 < \otimes_{NDVI}(x,y,t) \leq 0$). A few random pixels were detected within the urban area of Pomarico village, which, in the absence of any other information, can be considered as residual false positives; in any case, they are identified at lower confidence levels of the ALICE index.

While Figure 8 allowed us to follow the temporal evolution of the landslide, the output depicted in Figure 9 permits us to identify the whole area affected by the phenomenon in the February–November 2019 period. This map, indeed, describes the number of occurrences of anomalous ALICE values ($\otimes_{NDVI}(x,y,t) \leq -2$) on the basis of the images shown in Figures 6 and 8.

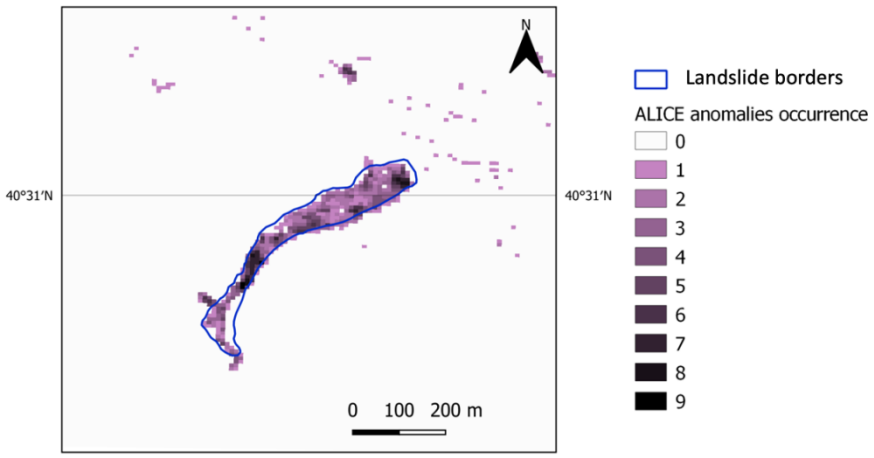

Figure 9. Map of occurrence of anomalous ($\otimes_{NDVI} \leq -2$) NDVI values.

The good agreement between the results achieved by the proposed methodology and in situ measurements is evident. Apart from a small subset in the landslide foot, almost the whole area within the blue vector has been identified at least once as anomalous by RST-cover, confirming its reliability. The "missed" area in the landslide foot is related to an area that, even if within the one affected by the phenomenon on the basis of the geological surveys, is characterized by not perturbed material [31]. This aspect is evident in analyzing the two RGB images in Figures 2 and 3, where the zone shows almost the same aspect and color. Two main clusters with a high number of occurrences are visible, one located towards the foot of the landslide and one on the landslide source area. The former is explainable as an accumulation zone, in which the soil flow conveys and remains stable for almost 2019, hence producing an evident perturbation for the whole sub-seasonal periods considered. The same reason is at the base of the large number of occurrences detected at the crown, where the fractures produced by the phenomenon may be identified as persistent scars of the initial land cover situation. Furthermore, further collapses of heavily damaged infrastructures might have occurred during the year, fostering the further identification of anomalous values. The persistent cluster of anomalous pixels, located in the north of the landslide, is associated with the surface transition during late 2018–early 2019, from resin to concrete, with a variation of NDVI values, of a tennis court there present, propaedeutic to the installation of tensile structure over it [45].

To summarize, a multitemporal approach based on the general RST methodology has been implemented on Sentinel-2 data to analyze its potential in identifying abrupt

land-cover changes due to a landslide that occurred in a small city (Pomarico) in South Italy. The GEE platform has been used to this aim, making the approach suitable to be easily exported wherever and applicable on a larger scale. Even if further analysis is needed to confirm such a possibility, also considering smaller landslides than the Pomarico one, preliminary results indicate the capability of the proposed approach to provide high-accuracy information not only just after the event but also in the following period. This would allow continuous monitoring of the area, useful for implementing adequate mitigation activities as well as providing early warning about possible further critical situations. Only after an extensive validation of the proposed technique, its application at large areas also to support landslide inventory compilation efforts, might be considered.

The quality of the achieved results will improve in the future by enlarging the analyzed dataset with the recent and continuous Sentinel-2 acquisitions, which will enhance the preliminary characterization of the expected values. Finally, it is worth noting that not all kinds of landslides could be detected by this approach. The basic requirement is the occurrence of a clear transition in land cover changes. For example, rockfall landslides affecting cliffs and steep slopes may be almost indistinguishable, both for the limitation of satellite observation for this kind of area, as well as for the poor difference in the land-cover which can be present before and after the event. A different indicator, more able to identify transitions that occur on soils that are poorly or not vegetated at all, such as the BSI, could be tested in this case.

Author Contributions: Methodology, V.T., V.S., and T.L.; software, V.S. and N.G.; formal analysis, V.S., E.C., C.F., and T.L.; writing—original draft preparation, V.S. and T.L.; writing—review and editing, V.T., E.C., and C.F.; supervision, V.T.; funding acquisition, V.T. All authors have read and agreed to the published version of the manuscript.

Funding: This research was supported by MIUR PON R&I 2014-2020 Program (project MITIGO, ARS01_00964).

Acknowledgments: the authors would like to thank Angela Perrone for the information provided about the main features of the Pomarico landslide.

Data Availability Statement: Publicly available datasets were analyzed in this study. This data can be found here: https://developers.google.com/earth-engine/datasets/catalog/COPERNICUS_S2.

Conflicts of Interest: The authors declare no conflict of interest.

References

1. Solari, L.; Del Soldato, M.; Raspini, F.; Barra, A.; Bianchini, S.; Confuorto, P.; Casagli, N.; Crosetto, M. Review of Satellite Interferometry for Landslide Detection in Italy. *Remote Sens.* **2020**, *12*, 1351. https://doi.org/10.3390/rs12081351.
2. Mateos, R.M.; López-Vinielles, J.; Poyiadji, E.; Tsagkas, D.; Sheehy, M.; Hadjicharalambous, K.; Herrera, G. Integration of landslide hazard into urban planning across Europe. *Landsc. Urban Plan.* **2020**, *196*, 103740. https://doi.org/10.1016/j.landurbplan.2019.103740.
3. Nesticò, A.; Maselli, G.; Russo, F. Hydrogeological Damage: An Overview on Appraisal Issues. In *New Metropolitan Perspectives*; NMP 2022. Lecture Notes in Networks and Systems; Calabrò, F., Della Spina, L., Piñeira Mantiñán, M.J., Eds.; Springer: Cham, Switzerland, 2022; Volume 482. https://doi.org/10.1007/978-3-031-06825-6_117.
4. Centre for Research on the Epidemiology of Disasters (CRED). Economic 1998–2017 Losses, Poverty & Disaster. Available online: https://www.preventionweb.net/files/61119_credeconomiclosses.pdf (accessed on 5 January 2023).
5. Haque, U.; Da Silva, P.F.; Devoli, G.; Pilz, J.; Zhao, B.; Khaloua, A.; Glass, G.E. The human cost of global warming: Deadly landslides and their triggers (1995–2014). *Sci. Total Environ.* **2019**, *682*, 673–684. https://doi.org/10.1016/j.scitotenv.2019.03.415.
6. Froude, M.J.; Petley, D.N. Global fatal landslide occurrence from 2004 to 2016. *Nat. Hazards Earth Syst. Sci*. **2018**, *18*, 2161–2181.
7. Crozier, M.J. Deciphering the effect of climate change on landslide activity: A review. *Geomorphology* **2010**, *124*, 260–267. https://doi.org/10.1016/j.geomorph.2010.04.009.
8. Guzzetti, F.; Polemio, M. Il rischio idrogeologico in Italia e il ruolo della ricerca scientifica.. Proceeding of "Dissesto Idrogeologico: Il pericolo geoidrologico e la gestione del territorio in Italia". Roma, 10 giugno 2011, publishe in Geologia dell'ambiente **2012**, Supp. *2, 7*. Available online: https://www.sigeaweb.it/documenti/gda-supplemento-dissesto-idrogeologico.pdf, (accessed on 23 January 2023).
9. Salvati, P.; Bianchi, C.; Rossi, M.; Guzzetti, F. Societal landslide and flood risk in Italy. *Nat. Hazard*., **2010**, *10*, 465–483.

10. Haque, U.; Blum, P.; da Silva, P.F.; Andersen, P.; Pilz, J.; Chalov, S.R.; Malet, J.P.; Auflič, M.J.; Andres, N.; Poyiadji, E.; et al. Fatal landslides in Europe. *Landslides* **2016**, *13*, 1545–1554. https://doi.org/10.1007/s10346-016-0689-3.
11. Perrone, A. Lessons learned by 10 years of geophysical measurements with Civil Protection in Basilicata (Italy) landslide areas. *Landslides* **2021**, *18*, 1499–1508. https://doi.org/10.1007/s10346-020-01584-3.
12. MITIGO. Mitigazione dei Rischi Naturali per la Sicurezza e la Mobilità nelle Aree Montane del Mezzogiorno. MIUR PON R&I 2014–2020 Program (Project MITIGO, ARS01_00964). Available online: https://www.mitigoinbasilicata.it (accessed on 23 January 2022).
13. Wasowski, J.; Bovenga, F. Remote sensing of landslide motion with emphasis on satellite multi-temporal interferometry applications: An overview. *Landslide Hazards Risks Disasters (Second Edition)* **2022**, 365–438. https://doi.org/10.1016/B978-0-12-818464-6.00006-8.
14. Lissak, C.; Bartsch, A.; De Michele, M.; Gomez, C.; Maquaire, O.; Raucoules, D.; Roulland, T. Remote Sensing for Assessing Landslides and Associated Hazards. *Surv. Geophys*. **2020**, *41*, 1391–1435. https://doi.org/10.1007/s10712-020-09609-1.
15. Handwerger, A.L.; Huang, M.-H., Jones, S.Y.; Amatya, P.; Kerner, H.R.; Kirschbaum, D.B. Generating landslide density heatmaps for rapid detection using open-access satellite radar data in Google Earth Engine. *Nat. Hazards Earth Syst. Sci*. **2022**, *22*, 753–773. https://doi.org/10.5194/nhess-22-753-2022.
16. Scheip, C.M.; Wegmann, K.W. HazMapper: A global open-source natural hazard mapping application in Google Earth Engine. *Nat. Hazards Earth Syst. Sci*. **2021**, *21*, 1495–1511. https://doi.org/10.5194/nhess-21-1495-2021.
17. Yang, W.; Wang, Y.; Sun, S.; Wang, Y.; Ma, C. Using Sentinel-2 time series to detect slope movement before the Jinsha River landslide. *Landslides* **2019**, *16*, 1313–1324 https://doi.org/10.1007/s10346-019-01178-8.
18. Deijns, A.A.; Bevington, A.R.; van Zadelhoff, F.; de Jong, S.M.; Geertsema, M.; McDougall, S. Semi-automated detection of landslide timing using harmonic modelling of satellite imagery, Buckinghorse River, Canada. *Int. J. Appl. Earth Obs. Geoinf.* **2020**, *84*, 101943. https://doi.org/10.1016/j.jag.2019.101943.
19. Wen, T.-H.; Teo, T.-A. Landslide inventory mapping from Landsat-8 NDVI time series using adaptive landslide interval detection. *ISPRS Ann. Photogramm. Remote Sens. Spat. Inf. Sci.* **2022**, *3*, 557–562. https://doi.org/10.5194/isprs-annals-V-3-2022-557-2022.
20. Rouse, J.W.; Haas, R.H.; Schell, J.A.; Deering, D.W. Monitoring vegetation systems in the Great Plains with ERTS. In Proceedings of the ERTS-1 Symposium 3rd, NASA, Greenbelt, MD, USA, 10–14 December 1974**.**
21. Gao, B.C. NDWI—A normalized difference water index for remote sensing of vegetation liquid water from space. *Remote Sens. Environ*. **1996**, 58, 257–266. https://doi.org/10.1016/S0034-4257(96)00067-3.
22. Ghorbanzadeh, O.; Didehban, K.; Rasouli, H.; Kamran, K.V.; Feizizadeh, B.; Blaschke, T. An application of sentinel-1, sentinel-2, and GNSS data for landslide susceptibility mapping. *ISPRS Int. J. Geo-Inf.* **2020**, *9*, 561.
23. Qu, F.; Qiu, H.; Sun, H.; Tang, M. Post-failure landslide change detection and analysis using optical satellite Sentinel-2 images. *Landslides* **2021**, *18*, 447–455. https://doi.org/10.1007/s10346-020-01498-0.
24. Qin, Y.; Lu, P.; Li, Z. Landslide inventory mapping from bitemporal 10 m sentinel-2 images using change detection based markov random field. *Int. Arch. Photogramm. Remote Sens. Spat. Inf. Sci.* **2018**, *42*, 1447–1452.
25. Psomiadis, E.; Papazachariou, A.; Soulis, K.X.; Alexiou, D.-S.; Charalampopoulos, I. Landslide Mapping and Susceptibility Assessment Using Geospatial Analysis and Earth Observation Data. *Land* **2020**, *9*, 133. https://doi.org/10.3390/land9050133.
26. Luti, T.; Segoni, S.; Catani, F.; Munafò, M.; Casagli, N. Integration of Remotely Sensed Soil Sealing Data in Landslide Susceptibility Mapping. *Remote Sens*. **2020**, *12*, 1486. https://doi.org/10.3390/rs12091486.
27. Ortonovi, S.; Bollot, N.; Pierre, G.; Deroin, J.P. Cartographie de la susceptibilité aux glissements de terraindans le vignoble champenois entre Epernay et Dormans (France): Apport de la télédétection multispectrale. *Géomorphologie Relief Process. Environ.* **2021**, *27*, 147–158. https://doi.org/10.4000/geomorphologie.15147.
28. Copernicus Web Site. Available online: https://www.copernicus.eu (accessed on 5 January 2023).
29. Tramutoli, V. Robust AVHRR Techniques (RAT) for environmental monitoring: Theory and applications. In *Earth Surface Remote Sensing II*; SPIE: Bellingham, WA, USA, 1998; Volume 3496, pp. 101–113.
30. Doglioni, A.; Casagli, N.; Nocentini, M.; Sdao, F.; Simeone, V. The landslide of Pomarico, South Italy, occurred on 29 January 2019. *Landslides* **2020**, *17*, 2137–2143. https://doi.org/10.1007/s10346-020-01455-x.
31. Perrone, A.; Canora, F.; Calamita, G.; Bellanova, J.; Serlenga, V.; Panebianco, S.; Tragni, N.; Piscitelli, S.; Vignola, L.; Doglioni, A.. A multidisciplinary approach for landslide residual risk assessment: The Pomarico landslide (Basilicata Region, Southern Italy) case study. *Landslides* **2021**, *18*, 353–365. https://doi.org/10.1007/s10346-020-01526-z.
32. Sdao, F.; Simeone, V. La grande frana di Pomarico del gennaio 2019–Risultati studi ed indagini–I Fase Emergenza. *Report for the Civil Protection Activities of the Municipality of Pomarico*, 2019.
33. Sassilive Website. Available online: https://www.sassilive.it/cronaca/istituzioni-cronaca/frana-di-pomarico-attivita-della-regione-basilicata-in-favore-della-popolazione/ (accessed on 3 January 2023).
34. Earth Engine Data Catalog. Available online: https://developers.google.com/earth-engine/datasets/catalog/COPERNICUS_S2 (accessed on 11 November 2022).
35. Tramutoli, V. Robust satellite techniques (RST) for natural and environmental hazards monitoring and mitigation: Theory and applications. In Proceedings of the 2007 International Workshop on the Analysis of Multi-Temporal Remote Sensing Images, Leuven, Belgium, 18–20 July 2007, pp. 1–6. https://doi.org/10.1109/MULTITEMP.2007.4293057.
36. Satriano, V.; Ciancia, E.; Lacava, T.; Pergola, N.; Tramutoli, V. Improving the RST-OIL algorithm for oil spill detection under severe sun glint conditions. *Remote Sens.* **2019**, *11*, 2762. https://doi.org/10.3390/rs11232762.

37. Lacava, T.; Ciancia, E.; Coviello, I.; Di Polito, C.; Grimaldi, C.S.; Pergola, N.; Tramutoli, V. A MODIS-based robust satellite technique (RST) for timely detection of oil spilled areas. *Remote Sens.* **2017**, *9*, 128. https://doi.org/10.3390/rs9020128.
38. Filizzola, C.; Carlucci, M.A.; Genzano, N.; Ciancia, E.; Lisi, M.; Pergola, N.; Ripullone, F.; Tramutoli, V. Robust Satellite-Based Identification and Monitoring of Forests Having Undergone Climate-Change-Related Stress. *Land* **2022**, *11*, 825. https://doi.org/10.3390/land11060825.
39. Ciancia, E.; Lacava, T.; Pergola, N.; Vellucci, V.; Antoine, D.; Satriano, V.; Tramutoli, V. Quantifying the Variability of Phytoplankton Blooms in the NW Mediterranean Sea with the Robust Satellite Techniques (RST). *Remote Sens.* **2021**, *13*, 5151. https://doi.org/10.3390/rs13245151.
40. Mazzeo, G.; De Santis, F.; Falconieri, A.; Filizzola, C.; Lacava, T.; Lanorte, A.; Marchese, F.; Nolè, G.; Pergola, N.; Pietrapertosa, C.; et al. Integrated Satellite System for Fire Detection and Prioritization. *Remote Sens.* **2022**, *14*, 335. https://doi.org/10.3390/rs14020335.
41. Lacava, T.; Greco, M.; Di Leo, E.V.; Martino, G.; Pergola, N.; Romano, F.; Sannazzaro, F.; Tramutoli, V. Assessing the potential of SWVI (Soil Wetness Variation Index) for hydrological risk monitoring by means of satellite microwave observations. *Adv. Geosci.* **2005**, *2*, 221–227. https://doi.org/10.5194/adgeo-2-221-2005.
42. Lacava, T.; Filizzola, C.; Pergola, N.; Sannazzaro, F.; Tramutoli, V. Improving flood monitoring by the Robust AVHRR technique (RAT) approach: The case of the April 2000 Hungary flood. *Int. J. Remote Sens.* **2010**, *31*, 2043–2062. https://doi.org/10.1080/01431160902942902.
43. Koeppen, W.C.; Pilger, E.; Wright, R. Time series analysis of infrared satellite data for detecting thermal anomalies: A hybrid approach. *Bull. Volcanol.* **2011**, *73*, 577–593. https://doi.org/10.1007/s00445-010-0427-y.
44. Di Polito, C.; Ciancia, E.; Coviello, I.; Doxaran, D.; Lacava, T.; Pergola, N.; Satriano, V.; Tramutoli, V. On the potential of robust satellite techniques approach for SPM monitoring in coastal waters: Implementation and Application Over the Basilicata Ionian Coastal Waters Using MODIS-Aqua. *Remote Sens.* **2016**, *8*, 922. https://doi.org/10.3390/rs8110922.
45. Sport & Impianti Website. Available online: https://www.sporteimpianti.it/notizie/tensostruttura-al-centro-sportivo-di-pomarico-matera/ (accessed on 5 January 2023).